ISBN: 978-3-95450-247-9 ISSN: 2673-5490 doi: 10.18429/JACoW-IPAC2024-MOPC14

A NEW BASELINE LAYOUT FOR THE FCC-hh RING

G. Pérez Segurana*, A. Abramov, W. Bartmann, M. Benedikt, R. Bruce, M. Giovannozzi, T. Risselada, F. Zimmermann, CERN, Geneva, Switzerland

Abstract

The Future Circular Collider (FCC) study includes two accelerators, a high-energy lepton collider (FCC-ee) and an energy-frontier hadron collider (FCC-hh). Both machines share the same tunnel infrastructure. We present the current status of FCC-hh design, highlighting the most recent changes, including a new layout following updated tunnel dimensions, a change from 12 to 16 dipoles per cell increasing the dipole filling factor, implementation of the beam-crossing scheme at experimental interaction points, and the optical solutions found for the eight experimental and technical insertions.

LAYOUT OF THE FCC-hh RING

Since the publication of the FCC Conceptual Design Report (CDR) [1] several studies have been carried out to provide a revised and improved version of the ring layout [2, 3]. The placement studies of FCC [4] provided strong indications that the length of the FCC rings had to be shortened, which was achieved primarily by reducing the lengths of the arcs.

The FCC-ee design introduced an important constraint because, to enable operation with four experimental insertions, the ring should assume a four-fold super-periodicity, with implications for the geometry of the FCC-hh ring. The functions of the various technical insertions had to be reviewed and merged differently. A radial displacement of the position of the interaction points (IPs) of the FCC-hh ring to coincide with the position of the IPs of the FCC-ee ring had to be implemented. The last part of the hadron transfer lines will be housed in the ring tunnel, which reduces the length of the tunnel needed for the transfer lines from the injector to the FCC(-hh) tunnel. Figure 1 presents the updated layout of the FCC-hh ring. The circumference length is 90.66 km, with technical insertions designed with a length of 2032 m and experimental insertions with a length of approximately 991 m. The experimental insertions (IRs) are located in Point A (PA), Point D (PD), Point G (PG) and Point J (PJ). Figure 2 (left) shows the geometric footprint of the two FCC-ee rings along with the average of the two FCC-hh rings, in the vicinity of PA.

Figure 2 (right) compares the three rings on the right side of an experimental insertion. The three rings converge towards the arc and are fully compatible with a single tunnel with enlarged cross section.

The injection of the clockwise beam is performed in PB and combined with the dump systems of both beams, whereas the injection of the counter-clockwise beam is performed in PL, combined with the RF system. The beams are always injected into the external channel of the FCC-hh accelerator. The collimation system is split into two insertions (each housing the systems for both beams): PF for betatron cleaning and PH for the momentum collimation system.

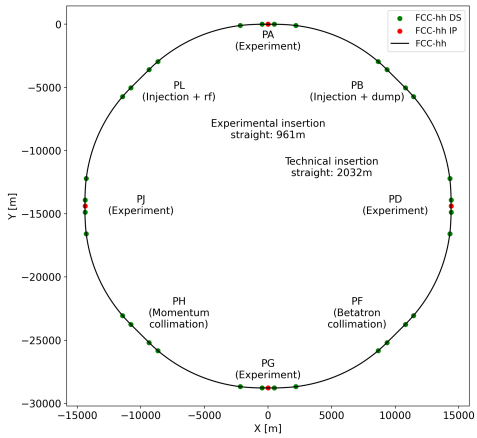

Figure 1: Layout of the new FCC-hh ring configuration.

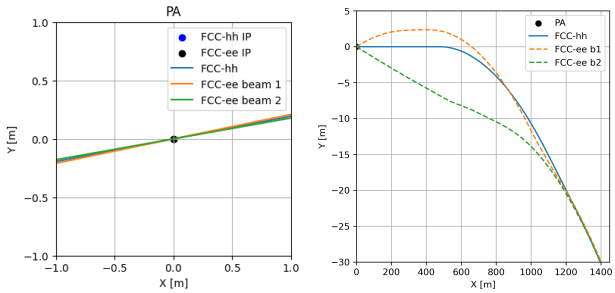

Figure 2: Left: View of the layout of the new FCC-hh ring configuration at the experimental insertion PA with the FCC-ee rings. Right: Comparison of the geometry of the FCC-hh ring and the two FCC-ee rings in the vicinity of PA.

In the CDR [1], a dipole field of 16 T was assumed, providing the centre-of-mass energy (100 TeV) for the then nominal circumference of the ring (97.75 km). The in-depth review of the FCC-hh layout led to considering two example values that span the full range of dipole fields under consideration, namely 14 T (to be realised with Nb_3Sn magnets) and 20 T (to be realised with high-temperature superconductor), which correspond to the centre-of-mass energies of 84.6 TeV and 120.8 TeV, respectively.

ARC DESIGN

With respect to the CDR solution, longer (approximately 276 m) regular cells with 16 dipoles have been used, leading to an increase in the dipole filling factor and an increase in the values of beta-functions and dispersion, that improves

* gustavo.perez.segurana@cern.ch

ISBN: 978-3-95450-247-9 ISSN: 2673-5490 doi: 10.18429/JACoW-IPAC2024-MOPC14

the efficiency of correction systems, such as chromatic sextupoles and Landau octupoles. The required beam aperture limits the cell length. The target aperture values, derived in Ref. [5], are 13.4 σ at the injection energy and 15.5 σ at the collision energy, where σ stands for the nominal rms beam size.

Dispersion suppressors (DS) were reviewed in depth, and their proposed layout is shown in Fig. 3, where both the DS connecting an arc and an experimental insertions (top) and the DS connecting an arc and a technical insertion (bottom) are shown.

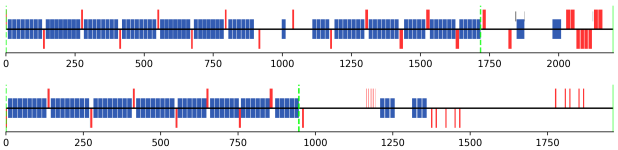

Figure 3: Layout of the dispersion suppressor also including half of the straight section for an experimental insertion (top) and for the straight section housing the momentum collimation at PH (bottom).

DSs are designed to control the dispersion and provide optical flexibility. The primary design challenge for the DS of the experimental insertions is the need to control the ring geometry by radially displacing the IPs. The quadrupoles of the DS are assumed to be powered independently for optical flexibility. This can be achieved by using main quadrupoles powered in series with the other regular arc quadrupoles, complemented by individually powered trim quadrupoles.

DSs for the technical insertions are shorter than those for the experimental insertions. Both types of DSs have short gaps (of the order of 2 m) to allow the installation of local DS collimators, which should absorb particles that have lost energy through interaction with the primary and secondary collimators [6].

EXPERIMENTAL STRAIGHTS

At the injection energy, $\beta^* = 10$ m, which is then reduced to $\beta^* = 30$ cm at collision energy. The squeeze of β^* will take place, at least partially, during the energy ramp, based on considerations of the available aperture.

The layout of the four experimental insertions is identical. However, the polarity of the separation and recombination dipoles changes between the insertions. This leads to small changes in the behaviour of the horizontal dispersion function that come in two variants. There are two important differences with respect to the layout presented in Ref. [1]: the straight section proper is about 991 m long instead of the former 1400 m, as a consequence of the radial displacement of the IP. Furthermore, the separation and recombination dipoles are superconducting, in line with the implementation for the HL-LHC [7, 8].

The optical parameters, dispersion, and aperture for the PD experimental insertion are shown in Fig. 4 at the injection energy with $\beta^* = 10$ m (left) and for the collision energy with $\beta^* = 30$ cm. The most striking difference is the maximum value of the beta-functions, which amounts to about 3000 m and 70 000 m for injection and collision optics, respectively.

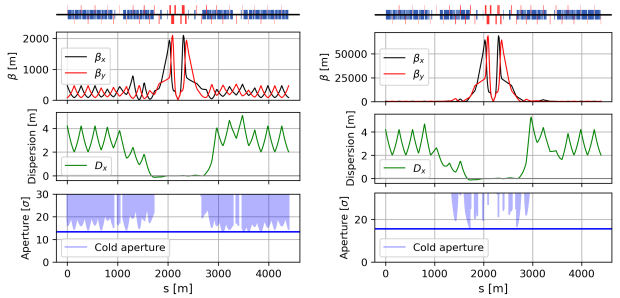

Figure 4: Optical parameters, dispersion, and beam aperture for the injection (left, $\beta^* = 10$ m) and the collision (right, $\beta^* = 30$ cm) optics of PD insertion. The aperture was computed with crossing angle and separation bumps.

BEAM DUMP AND INJECTION STRAIGHT

The injection system envisages a bunch-to-bucket transfer [1], while the dump system is externally triggered and extracts, dilutes, and absorbs the entire beam on an external absorber, located 2.5 km from the extraction point in a dedicated cavern. The design of the complete dump system is driven by considerations of machine protection [9]. The new layout imposes an overlap of the two systems, with the most restrictive phase advance constraints between the respective kickers and the corresponding protection absorbers, shown in Fig. 5. The injection system is upstream, with a septum

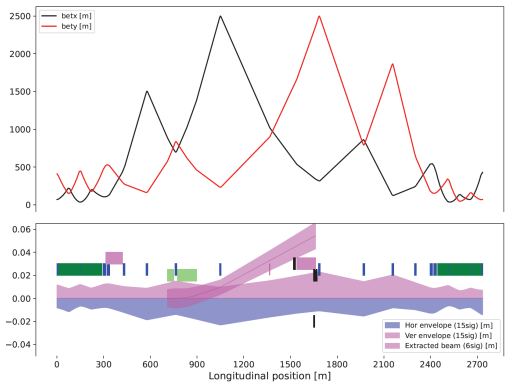

Figure 5: Optics (top) and beam envelopes and active elements (bottom) for the injection and extraction straight section around PB.

magnet placed in the first available drift, at 90° phase advance, and two quadrupoles downstream of the injection kicker. Both the injection and dump systems deflect the beams in the vertical plane. The extraction kicker is next to the injection one, separated by a quadrupole, and both kicker systems share the overall straight-section optics, with a long drift towards their respective protection absorbers, again separated by 90° of phase advance.

ISBN: 978-3-95450-247-9 ISSN: 2673-5490 doi: 10.18429/JACoW-IPAC2024-MOPC14

The extraction system had to be squeezed into the reduced length of the straight section. This caused an increase in the length of the superconducting extraction septa, the switch voltage, and the length of the extraction kickers system. To mitigate these technological challenges, the beams could be extracted through a hole in the cryostat of the downstream quadrupole, reducing the septum deflection by about a third.

The technological challenges posed by the machine protection aspects for the combined injection and beam dump systems suggest that an alternative solution should be considered. One could envisage housing the dump systems in PF and the betatron collimation system in PH, and merging the injection of the clockwise beam with the momentum collimation system at PB. This scenario will be studied in detail in the near future.

COLLIMATION STRAIGHTS

Two new features have been implemented in the collimation insertions: a new dogleg geometry to ease the design of the normal-conducting dipoles, and a constant inter-beam distance along the whole straight insertion to implement the same optical and dispersion functions for both beams.

The momentum collimation system is located in PH, and the layout and optics are shown in Fig. 6 (left). The beam aperture is plotted for the injection energy, which represents the most stringent situation, since the same optics is assumed at top energy.

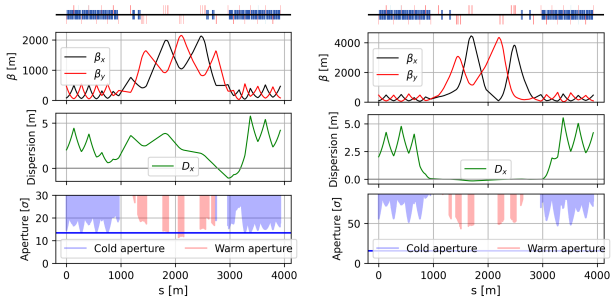

Figure 6: Optical parameters, dispersion, and beam aperture for the optics of PH (left) and PF (right). The blue and red aperture regions indicate superconducting and normal-conducting magnets, respectively (the target aperture is mandatory only for superconducting magnets).

The betatron collimation system is located in PF. A novel optical configuration [10] with high-beta values was designed to mitigate the impedance generated by the collimators, following the approach pursued for the LHC and HL-LHC [11, 12]. This optics is suitable for top energy only; consequently, two optics were designed: one with mid-range values of the beta-function for injection energy and one with large values of the beta-functions for collision energy, shown in Fig. 6 (right). An optical transition between the two configurations is needed during the energy ramp.

RF AND INJECTION STRAIGHT

The RF system and the injection of the counter-clockwise beam are located in PL. The RF system, installed downstream of the injection system, imposes an increased inter-beam distance and cancellation of the dispersion in the part of the straight section where the cavities are located. These constraints are met by means of two achromatic doglegs.

The injection system shall inject the beam by acting on the vertical plane only, since the transfer lines will run above the main ring magnets, just on top of the circulating beam. The regular cell of the transfer line is assumed to be the same as for the circulating beam, which ensures the same optical parameters. An additional constraint is to use the same hardware as installed in PB.

The optics of the counter- and clockwise beams are shown in Fig. 7 (left) and (right), respectively. The injection system is located close to the DS on the right-hand side. This part is left empty here, as the injection elements are inactive for the circulating beam.

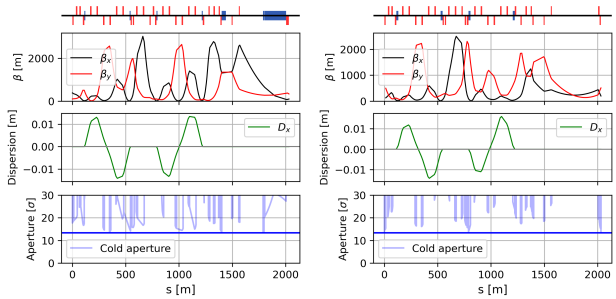

Figure 7: Optical parameters, dispersion, and beam aperture at injection for the optics of the RF and injection insertion for the counter- (left) and clock-clockwise beam (right). Note that in the left plot the beam travels right to left.

CONCLUSIONS AND OUTLOOK

A new baseline lattice was developed for the CERN Future hadron Circular Collider. With a circumference of approximately 91 km and a centre-of-mass energy of, e.g. 96 TeV for a dipole field of 16 T, the lattice is compatible with higher collision energies, considering HTS or HTS-hybrid magnets with a dipole field of up to 20 T.

The layout of the various insertions is the result of an in-depth review of the original configuration presented in the FCC-hh CDR and of that of the FCC-ee, with several major novelties implemented and adaptation to the optimised FCC placement and layout.

A critical point is the combination of injection and dump systems in PB, in view of machine protection considerations with regard to combined failures. A possible mitigation would be separating these two systems and re-allocating the technical insertions, so that PB would house the injection of the clockwise beam and momentum collimation systems; PF the beam dumps systems; PH the betatron collimation systems. This work is currently underway.

ISBN: 978-3-95450-247-9 ISSN: 2673-5490 doi: 10.18429/JACoW-IPAC2024-MOPC14

REFERENCES

[1] A. Abada *et al.*, "FCC–hh: The Hadron Collider: Future Circular Collider Conceptual Design Report Volume 3. Future Circular Collider," *Eur. Phys. J. Spec. Top.*, vol. 228, pp. 755–1107, 2019. doi:10.1140/epjst/e2019-900087-0

[2] M. Benedikt *et al.*, "Status and challenges of the Future Circular Hadron Collider FCC-hh," in *Proceedings of 41st International Conference on High Energy physics — PoS(ICHEP2022)*, vol. 414, 2022, p. 058. doi:10.22323/1.414.0058

[3] M. Giovannozzi *et al.*, "Recent updates of the layout of the lattice of the CERN hadron-hadron Future Circular Collider," in *Proc. IPAC'23*, Venice, Italy, 2023, pp. 598–601.

[4] J. Gutleber, P. Laidouni, V. Mertens, *et al.*, *Synthèse des contraintes et opportunités d 'implantation du Futur Collisionneur Circulaire (FCC)*, version 2.0, 2023. doi:10.5281/zenodo.10369593

[5] R. Bruce and J. Molson, "Preliminary collimation system design concept and performance estimate: Deliverable D2.6," CERN, Tech. Rep., 2019, On behalf of EuroCirCol WP2. https://cds.cern.ch/record/2665192

[6] S. Redaelli, R. Bruce, A. Lechner, and A. Mereghetti, "Chapter 5: Collimation system," *CERN Yellow Rep. Monogr.*, vol. 10, pp. 87–114, 2020. doi:10.23731/CYRM-2020-0010.87

[7] O. Brüning and L. Rossi, "The High-Luminosity Large Hadron Collider," *Nat. Rev. Phys.*, vol. 1, no. 4, pp. 241–243, 2019. doi:10.1038/s42254-019-0050-6

[8] I. Béjar Alonso, O. Brüning, P. Fessia, L. Rossi, L. Tavian, and M. Zerlauth, *High-Luminosity Large Hadron Collider (HL–LHC): Technical design report*. CERN, 2020. doi:10.23731/CYRM-2020-0010

[9] W. Bartmann *et al.*, "Dump system concepts for the future circular collider," *Phys. Rev. Accel. Beams*, vol. 20, p. 031 001, 3 2017. doi:10.1103/PhysRevAccelBeams.20.031001

[10] A. Abramov, R. Bruce, M. Giovannozzi, G. Perez-Segurana, S. Redaelli, and T. Risselada, "Collimation system for the updated FCC-hh design baseline," in *Proc. IPAC'23*, Venice, Italy, 2023, pp. 352–355.

[11] R. Bruce, R. D. Maria, M. Giovannozzi, N. Mounet, and S. Redaelli, "Optics Configurations for Improved Machine Impedance and Cleaning Performance of a Multi-Stage Collimation Insertion," in *Proc. IPAC'21*, Campinas, Brazil, May 2021, 2021, pp. 57–60. doi:10.18429/JACoW-IPAC2021-MOPAB006

[12] B. Lindström *et al.*, "Settings for Improved Betatron Collimation in the First Run of the High Luminosity LHC," in *Proc. IPAC'22*, Bangkok, Thailand, 2022, pp. 1366–1369. doi:10.18429/JACoW-IPAC2022-TUPOTK062